Quaternary ammonium compounds to prevent oral biofilm formation

Miura Sugii, Mari

3

Chapter 3

Physical, chemical and antimicrobial evaluation of a composite material containing quaternary ammonium salt for braces cementation

Mari Miura Sugii; Fábio Augusto de Souza Ferreira; Karina Cogo Müller; Debora Alves Nunes Leite Lima; Ubirajara Pereira Rodrigues Filho; Flávio Henrique Baggio Aguiar

(Reprinted with the permission of Elsevier from Mater. Sci. Eng. C. 2017, 10.1016/j.msec.2016.12.084)

ABSTRACT

The antibiofilm effect of iodide quaternary ammonium methacryloxy silicate (IQAMS) in Transbond XT Light Cure Adhesive resin used for braces cementation was evaluated. Fourier Transform Infrared (FTIR) spectroscopy confirmed IQAMS formation and Scanning Electron Microscopy coupled to Energy-Dispersive X-ray Spectroscopy (SEM-EDS) revealed that as coating, the quaternary ammonium groups from IQAMS were homogeneously dispersed throughout the surface. When incorporated, the composite material presented homogeneous dispersion throughout the resin. Assays with *Streptococcus mutans* demonstrated enhanced antibiofilm effect for the IQAMS coated resin, with much lower colony-forming units (CFU), in comparison to incorporated IQAMS. Such a difference was assigned to low availability of quaternary ammonium groups at the surface of resin when IQAMS was incorporated, hindering its antibacterial effect. Additionally, the incorporation of IQAMS led to slightly decrease in ultimate bond strength (UBS) and shear bond strength (SBS), in comparison to neat resin. Thus, the synthesized IQAMS displays great potential as antibiofilm coating or sealant to prevent oral infections in brackets during orthodontic treatment.

INTRODUCTION

The goal of orthodontic treatment is to provide complete and integrated therapy for patients' oral health; restoring function as well as aesthetics [1–3]. Many orthodontic treatments available involve cementation of brackets and other metallic devices combined with elastic ligatures and arc wires, hindering hygiene. This results, for instance, in large *Streptococcus mutans* [4,5] and *Candida albicans* [6] biofilm accumulation and colonization, which it can lead to dental caries, compromising the oral health of patients [1,7–9]. The prevention of dental caries requires commitment and effort of the patient to properly cleanse the orthodontic devices, in addition to make use of a less cariogenic diet [10]. In order to support the patients and become the orthodontic treatment more effective, researchers have developed new materials with antimicrobial (bactericidal/bacteriostatic) properties [11,12].

Organically modified silicates (ORMOSIL) are hybrid materials [13] that contain organic functionalities covalently bonded to the silicate network providing especial properties [14,15]. Sol-gel process is a suitable approach to obtain ORMOSIL-based materials under mild conditions with multifunctional properties [13,14,16–18]. In a typical sol-gel process, silicon alkoxides precursors undergo acid or basic-catalyzed hydrolysis forming silanol groups (Si–OH) that further react to form siloxane bonds (Si–O–Si) and hence lead to the development of a tridimensional network [13,17,18]. Given its low toxicity and biocompatibility, ORMOSIL have been used as biomaterial by immobilization of biomolecules or modification of the silicate network with functional groups with biological properties [16,18,19]. Among the functional groups, the quaternary ammonium salts are known antimicrobial compounds, used as disinfectant in food production and medical appliances to prevent contamination and bacterial infections [20]. In this regard, dimethyloctadecyl[3-(trimethoxysilyl)propyl] ammonium chloride, an ORMOSIL precursor, has emerged as an effective compound for development antibacterial dental composites [19,21–24].

The antimicrobial activity of the quaternary ammonium groups is attributed to their ionic part combined to a lipophilic chain [25]. Palermo et al. found that the alkyl chain can penetrate into the cell causing lysis and death [26]. Li et al. [27] showed a large decrease of colony-forming unity (CFU) on samples containing quaternary ammonium groups with 12 carbons length. Additionally, Gong et al. [28] observed that the modification of the ORMOSIL network with methacrylate

groups led to development of quaternary ammonium methacryloxy silicates (QAMS), that incorporated and dispersed better in the orthodontic resin by establishment of covalent bonds via copolymerization with the acrylate groups present in the orthodontic resin [19,24,28].

Based on the previous statements, this study focused in the synthesis of iodide quaternary ammonium methacryloxy silicate (IQAMS) and evaluation of its antibiofilm properties, in the presence of *Streptococcus mutans*, when it was applied as coating or incorporated in different concentrations into Transbond XT Light Cure Adhesive resin for braces cementation. The chemical and physical properties of the materials obtained were also evaluated.

EXPERIMENTAL

Materials

(3-Iodopropyl)trimethoxysilane (IPTMS, Sigma-Aldrich, ≥95%), N,N-Dimethyldodecylamine (DMDA, Sigma-Aldrich, 97%), Tetraehtyl orthosilicate (TEOS, Sigma-Aldrich, 98%), 3-(Trimethoxysilyl)propylmethacrylate (TMSPM, Sigma-Aldrich, 98%), Hydrochloric acid (HCl, J.T. Baker, 36.5-38%), ultrapure water deionized water and N,N-Dimethylformamide (DMF, Sigma-Aldrich, 99.8%). All compounds were used as purchased.

Synthesis, deposition and incorporation of IQAMS in Transbond XT Light Cure resin

The synthesis of IQAMS followed two steps:

In *step 1*, a round-bottomed 50 mL flask was protected from light and put into silicone oil bath. Then, 25 mL of DMF were added, followed by addition of 1158 μL of IPTMS and 1753 μL of DMDA. A condenser was attached to the flask and the solution was put under stirring and heated up to 110 °C and kept it for 24 h under reflux. A scheme of step 1 is presented in Fig. 1.

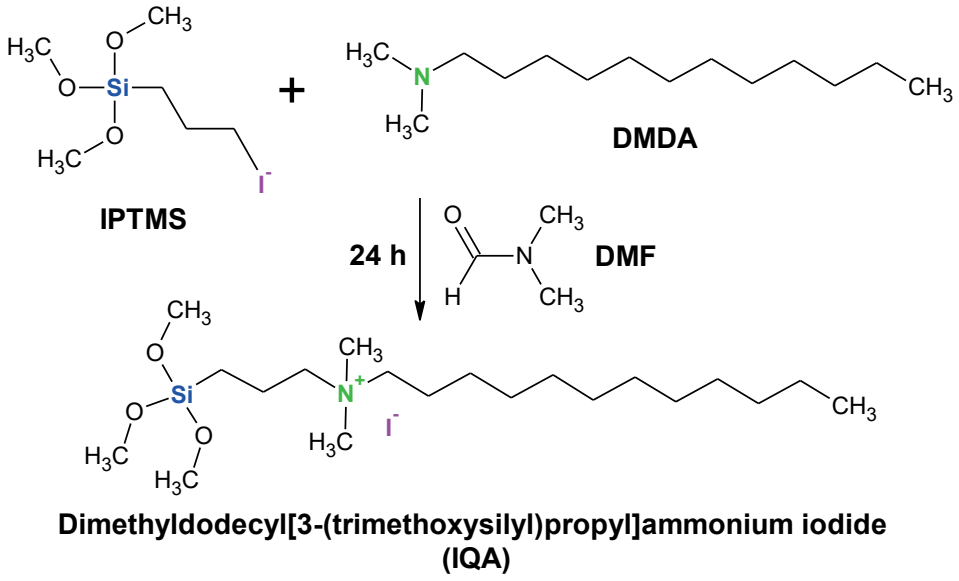

Figure 1. Schematic representation of step 1.

In *step 2*, after 24 h, still under stirring, the heating was turned off and once the temperature reached 25 °C, the condensation system was removed and 646 µL of TEOS were added and after 5 min, 714 µL of TMSPM. Then, 15 min later, 700 µL of HCl 0.3 mol L^{-1} were added to catalyze the hydrolysis and condensation process of the alcoxysilanes initiating the formation of the ORMOSIL network. The reaction proceeded for 1 h when the stirring was turned off. A scheme of step 2 is presented in Fig. 2.

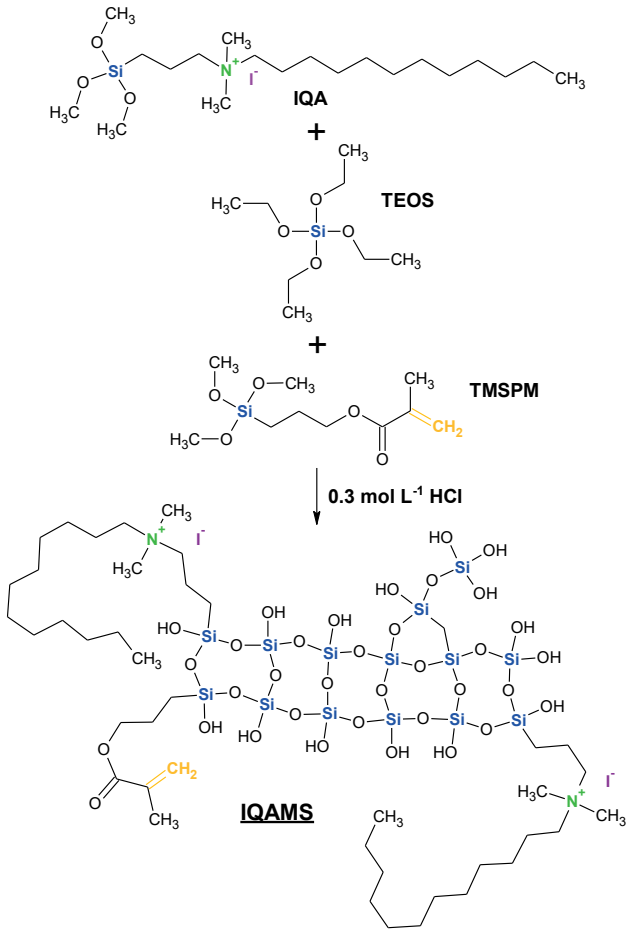

Figure 2. Schematic representation of step 2.

The solution containing the IQAMS was transferred to a Teflon® mold and taken to a pre-heated furnace at 80 °C to evaporate the solvent for 48 h. The solid obtained product was put in a Soxhlet extractor depurated in ethanol for 24 h and then rota-evaporated. All these procedures were to ensure the quality of the product.

For the incorporation, the IQAMS, obtained in the form of a viscous gel, was dispersed in 2 mL of ethanol and mixed to 11 g of Transbond XT composite resin (3M ESPE) using the Speed Mixer™ Laboratory Mixer System (Synergy Devices Limited). Two different volumes of solution were used and the groups obtained are presented in Table 1.

Table 1. Groups and correspondent IQAMS percentage and volume used.

Group	wt% of IQAMS in the composite resin	Volume of IQAMS solution (mL)
T	0	0
T10	10	735.7
T15	15	1103.6

A fourth group named TC, where C stands for coating, was obtained from application of 2 layers of IQAMS on the resin using disposable applicators (Microbrush).

Characterization techniques

*Chemical structure: Fourier transform infrared spectroscopy in transmission mode (*T-FTIR*)* was performed in a SHIMADZU IRA-affinity-1 spectrometer in the range of 4000-650 cm^{-1} with a spectral resolution of 4 cm^{-1}. The samples were dispersed into potassium bromide (KBr) and pressed as pellets. Neat KBr pellet was used as background. FTIR in Attenuated Total Reflectance mode (ATR-FTIR) was performed in a PERKIN ELMER spectrometer operating in the range of 1665 cm^{-1} to 1580 cm^{-1} with a spectral resolution of 4 cm^{-1}. Air was used as background.

Scanning Electron Microscopy (SEM): SEM was performed in a ZEISS LEO 440 microscope with OXFORD 7060 detector operating with 15 kV electron beam, current of 2.82 pA and I probe of 200 pA. The samples were previously coated with carbon by using BAL-TEC 020 sputter system. *Energy-Dispersive X-ray Spectroscopy (EDX)* was performed in a EDX LINK ANALYTICAL equipment, coupled to ZEISS LEO 440, with Pentaflet SiLi detector, ultrathin window ATW II from 133 eV to 5.9 keV resolution. Cobalt (Co) was used for calibration, electron beam of 15 kV, focal distance of 25 mm, dead time of 30%, current of 2.82 A and I probe of 2.5 nA. Each mapping was obtained by taking 40 frames.

Degree of Conversion (DC): DC was evaluated for the three groups (n=7) presented in Table 1 using ATR-FTIR. The initial measurement was performed on a non-polymerized resin. Subsequent measurements were performed on photo cured samples using a Valo LED from Ultradent Products Inc., on standard mode, with irradiance of 1000 mW cm^{-2} for 20 s irradiated directly on ATR crystal. For each sample, 16 scans were collected. The DC was calculated based on the aliphatic carbon bond and aromatic carbon bond ratio, representing the non-polymerized and polymerized states, respectively [29,30].

Water Sorption (Wsp) and Solubility (Wsl): Samples were prepared in a circular Teflon® matrix with 5 mm diameter and 1 mm depth. A polyester strip was placed under Teflon® mold and resin inserted in a single step. Another polyester strip and a glass slide were placed above the filled matrix and finger pressure was applied for 10 s to remove excess of material, leaving a flat surface. Then, the glass slide was removed and the composite was photocured for 20 s using a third generation Valo LED on standard mode. After 24 h, the specimens were stored in dissector containing silica gel, at 37 °C. Discs were weighed on analytical balance (Tel Marke, Bell Quimis) with 0.0001 g accuracy until constant weight **m1** was obtained (weight loss no greater than 0.0001 g/24 h). Sample thickness was measured at 4 different regions and the diameter was measured at two locations using a digital caliper (Mitutoyo). The average diameter and thickness were used to calculate the volume. The samples were individually stored in 2 mL of distilled water at 37 °C for 7 days. Then, the samples were rinsed, carefully dried with absorbent paper and weighed to obtain **m2**. Subsequently, the specimens returned to the dryer and and once the mass became it constant, **m3** was achieved. Sorption and solubility values were recorded in g mm^{-3} and calculated using the following equations: $\mathbf{W_{sp}=(m2-m3)/V}$ and $\mathbf{W_{sl}=(m1-m3)/V}$.

Ultimate Bond Strength (UBS): For each experimental group in Table 1, 7 specimens (10 mm length x 1 mm wide x 1 mm thick) were prepared using silicone matrix (Express XT, 3M ESPE). Polyester strip and glass plate were placed on top of the matrix and finger pressure was applied for 10 s. The specimens were then photocured for 20 s using Valo LED at standard mode. After 24 h, the specimens were fixed to a metallic device using cyanoacrylate glue (Super Bonder, LOCTITE HENKEL CORPORATION) and taken to the 441 INSTRON universal testing machine to test the cohesive strength at 0.5 mm min^{-1} speed. The cohesive strength was calculated according to: **RC=F/A**, where F is the tensile force in Newtons (N) and A the cross section area of the sample (mm^2). The values were expressed in Mega Pascal (MPa).

Shear Bond Strength (SBS): Thirty bovine incisors were extracted and stored in aqueous solution of 0.1% buffered thymol (Dinâmica). Remaining tissues were removed using Duplex periodontal curettes (SS White) and the teeth were polished using rubber cup polish (KG Sorensen Ind. Com Ltda) and pumice paste. After cleaning, the teeth were stored in distilled water at 37 °C. A doubled-faced diamond disc (KG Sorensen) was used to separate the crown from the root under

constant irrigation in a low speed handpiece. Cuts were made with a diamond disc 4"x012x1/2 (BUEHLER) in mesio-distal and cervico-incisal directions in a metallographic cutting machine (BUEHLER Isomet 1000) to obtain 25 mm^2 blocks with an enamel surface. Each fragment was included in polystyrene resin and ground flat using sandpaper (#600 and #1200) under constant irrigation in polishing machine (AropolE Arotec). Then, the samples were cleaned in ultrasonic bath (Marconi) for 10 min to remove debris. Incisor Edgewise Standard metallic brackets (Morelli) were cemented on the specimens in accordance with Transbond XT Light Cure manufacture instructions. For bonding procedures, each specimen was etched using 35% phosphoric acid (Ultra EtchTM – Ultradent Products Inc.) for 30 s. Each surface was abundantly rinsed and gently dried with airflow. The Transbond XT Primer was applied and photocured for 20 s. Subsequently, a small amount of composite was applied directly to the base of the bracket. The bracket was then positioned on the block surface and gently pressed to remove excess material. Photoactivation was performed on each side of the bracket for 20 s with Valo LED at Standard mode. Specimens were stored in distilled water for 24 h at 37 °C before shear bond testing. The brackets were removed using a chisel connected to Instron universal testing with 5 kg load cell at crosshead speed of 0.5 mm min^{-1}.

Streptococcus mutans biofilm formation assay: The test used the experimental groups described in section 2.2. For each experimental group, 6 samples with 5 mm diameter and 2 mm depth were prepared according to procedure described in section 2.3.4. After 24 h, all samples were sterilized using γ radiation. Biofilms of *S mutans* UA 159 were formed on the composite resin discs. The Bacteria were kept in freezer at -80 °C in Brain Heart Infusion (BHI, Difco Co.) containing 20% glycerol solution (V/V). The bacteria inoculum was prepared from overnight culture using BHI broth supplemented with 1% sucrose and adjusted to optical density of 0.7 (wavelength of 660 nm≈$1x10^{-9}$ CFU mL^{-1}). From this inoculum, $4x10^6$ CFU mL^{-1} were transferred to each cell of 24 h polystyrene culture plate that contained 3 mL of BHI and 1% sucrose. Samples were placed in vertical position into each well and they were incubated for 24 h at 37 °C in 5 % CO_2. Then, specimens were removed from the plates and washed 5 times in 3 mL sterile saline. Each specimen was transferred to a tube containing 5 mL of sterile saline and the biofilm was detached after 1 min in vortex mixer followed by sonication (Vibra Cell 400w, Sonic & Materials Inc) with 5% amplitude and 6 pulses (9.9 s each and 5 s interval). Then, 10 μL of the biofilm suspension was placed on BHI agar and incubated for 48 h. After incubation, the number of colony-forming units per

milliliter of suspension (CFU mL^{-1}) was determined. Statistical analysis of CFU mL^{-1} was subjected to non-parametric Kruskal-Wallis and Student-Newman-Keules tests (a=0.05).

DC, UBS and SBS were subjected to one-way ANOVA and Tukey's post hoc test (a=0.05).

RESULTS AND DISCUSSION

Structural characterization

T-FTIR analysis of synthesized IQAMS is shown in Fig. 3. Peaks in the 1000-1200 cm^{-1} region were assigned to the siloxane bonds (Si–O–Si), while above 3000 cm^{-1} and around 880 cm^{-1} were due to the silanol groups (Si–OH) [31,32]. Regarding to the aliphatic chain and quaternary ammonium groups, their characteristic bands were observed in the range of 3000-2800 cm^{-1} related to C–H, and at 1640 cm^{-1} and at 1470 cm^{-1}, assigned to the methacrylate and quaternary ammonium groups $–N^{+}(CH_3)_2(C_{12}H_{25})$ [31–34]. These bands confirmed the IQAMS formation and efficiency of the synthesis procedure used. The material obtained was viscous, yellow and sticky.

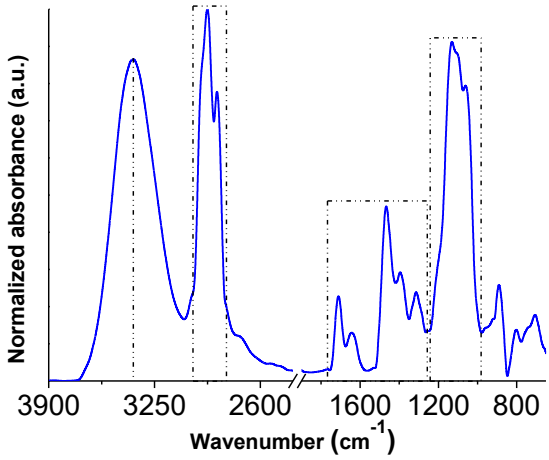

Figure 3. T-FTIR analysis of the synthesized IQAMS.

Compositional and morphological analysis

From SEM images and EDX mapping analysis (Fig. 4), it was possible to identify Si (K_α=1.740 keV) and I (L_α=3.937 keV). In the neat resin, Si was related to the silica particles used as filler, while in IQAMS Si was related to the ORMOSIL network developed and I, in the form of iodide (I^-), was the counterion of the

quaternary ammonium group. Note that similar mapping was obtained for the as-prepared and coated IQAMS. Silica particles were no longer observed on the coated resin. The shrunken-like morphology observed for the IQAMS coating is due to the intensity of the electron beam.

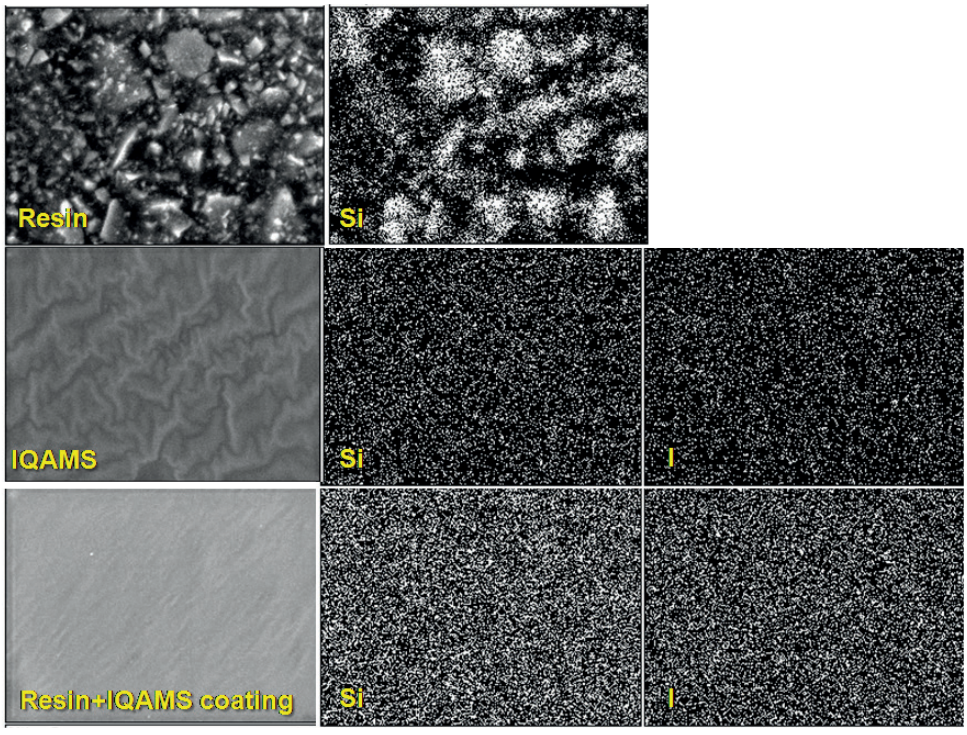

Figure 4. On top: SEM image of composite resin Transbond XT with respective Si EDX mapping. In between: SEM image of as-prepared IQAMS hybrid material with respective Si and I EDX mapping. At bottom: SEM image of the resin with 2 layers of IQAMS with respective Si and I EDX mapping.

DC, UBS and SBS assays

According to ATR-FTIR, the incorporation of IQAMS into commercially available composite resin Transbond XT Light Cure had no effect on DC, in comparison with neat resin. From Table 2, DC was similar in all tested groups ($p>0.05$). Additionally, the dispersion of IQAMS into 2 mL of ethanol, before its incorporation, may have caused the decrease in interfacial adhesion between the resin matrix and the silica particles used as load, so that during mechanical tests these regions became stress concentration zones leading to adhesive and cohesive failure [35,36]. Furthermore, the acrylate coupling agent groups present in IQAMS structure and the acrylate groups present in Transbond XT Light Cure composite

resin may also have chemically interacted poorly with each other [37]. Regarding to W_{sp} and W_{sl}, as the amount of IQAMS incorporated increased, both decreased ($p<0.05$), as expected, since the 12 carbons alkyl chain present in the IQAMS structure assigned a hydrophobic character to the material [12] reflecting in lower solubility and water intake.

Table 2. Means values and Standard Deviations of UBS, SBS, DC W_{sp} and W_{sl}.

Groups	UBS (Kg F^{-1})	SBS (N)	DC (%)	W_{sp} (g mm^{-3})	W_{sl} (g mm^{-3})
T	5.39 (±1.53) a	6.08 (±2.01) a	42.88 (±1.02) a	0.0429 (±0.0008) a	0.0427 (±0.0007) a
T10	3.80 (±0.88) b	4.75 (±2.23) a	43.50 (±1.36) a	0.0397 (±0.0008) b	0.0394 (±0.0008) b
T15	1.12 (±0.45) c	2.12 (±0.7) b	43.73 (±1.71) a	0.038 (±0.0004) c	0.0377 (±0.0003) c

Different letters are statistically different (in columns) ($p<0.05$).

Streptococcus mutans biofilm formation assay

Fig. 5 presented the amount of biofilm formed during the microbial assays. The data demonstrated that the neat and IQAMS-incorporated resin presented similar results toward *S. mutans* with higher CFU in comparison to IQAMS-coated resin ($p<0.05$). Such behavior was assigned to the lack of IQAMS on the surface of the samples when incorporated, resulting in poor activity against biofilm formation. However, when it was applied as coating, the quaternary ammonium groups from IQAMS could then properly reveal its antibiofilm effect. The large deviation obtained for TC is due to higher CFU presented for 1 of the 6 samples analyzed. In Fig. 6 is an illustrative representation of incorporated and coated IQAMS. Note that in the later, the quaternary ammonium groups are properly exposed.

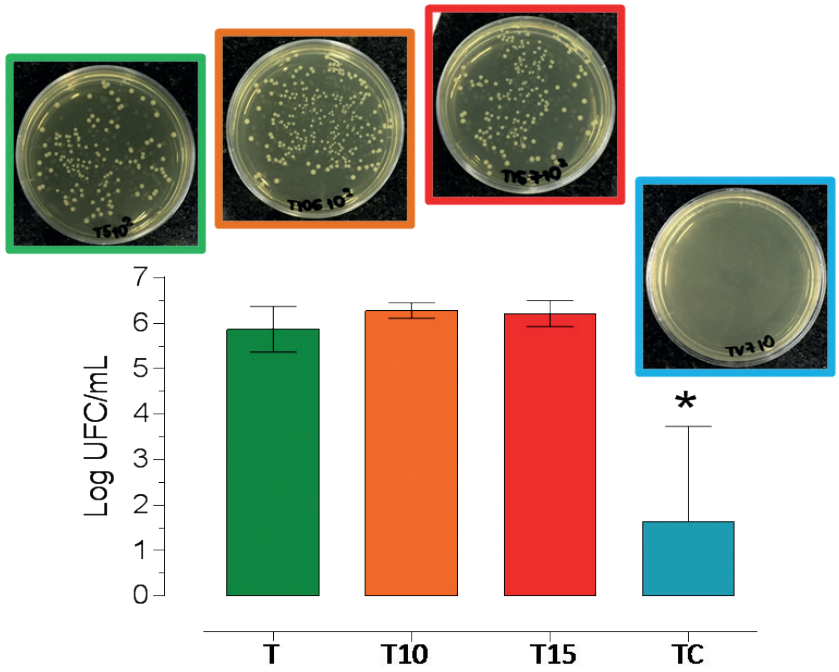

Figure 5. Means and Standard deviation of log CFU mL^{-1} of groups T, T10, T15 and TC.

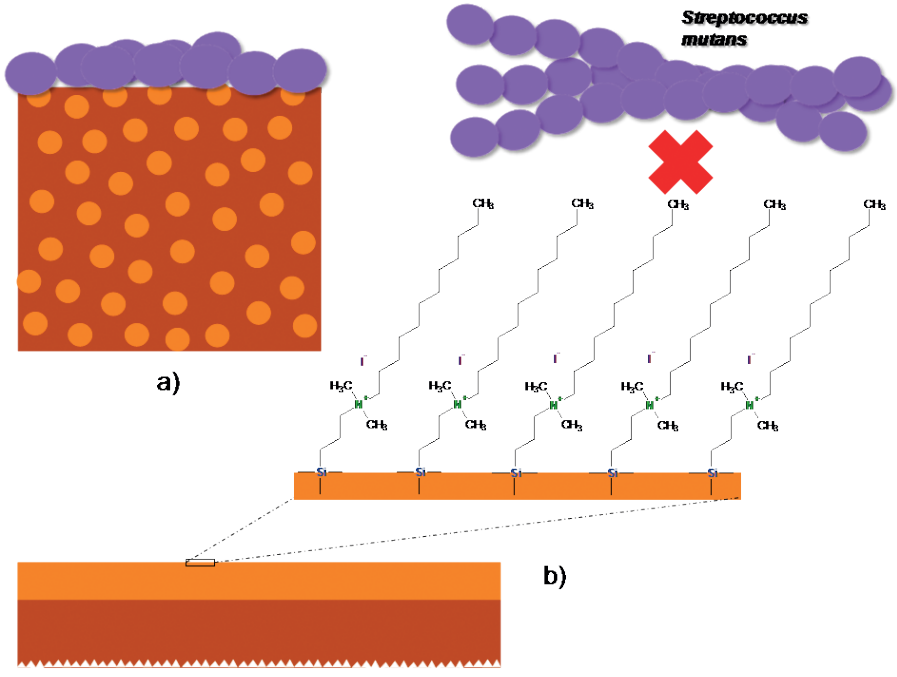

Figure 6. Illustrative representation of (a) incorporated and (b) coated IQAMS.

CONCLUSIONS

The synthesis of IQAMS hybrid material was properly performed and revealed antibiofilm activity against *Streptococcus mutans* biofilm formation. Nevertheless, the IQAMS incorporation into the commercial composite resin Transbond XT Light Cure hindered its antibacterial activity in addition to decrease UBS and SBS resistance of the resin. In contrast, when it was applied as coating, the material presented a positive perspective for development of varnishes and sealants with antimicrobial activity. Dental materials with such properties are important to support preventing caries during orthodontic treatment. The results found are promising and further studies will be conducted to evaluate the interaction between the acrylate groups from IQAMS and resin, the clinical relevance toward adverse conditions and long-term exposition to bacterial environments as well as to assess the endurance of the material under tooth brushing and saliva.

ACKNOWLEDGEMENTS

The authors acknowledge the financial support from CNPq (Grant. 142910/2010-4) and FAPESP (CEPID 2013/07793-6 and Grant. 2013/15518-5). We also extend acknowledgements to the group of Química de Materiais Híbridos e Inorgânicos (GQMatHI) from Instituto de Química de São Carlos (IQSC) for all technical support provided.

REFERENCES

[1] Yagci A, Korkmaz YN, Buyuk SK, Yagci F, Atilla AO. White spot lesion formation after treatment with full-coverage rapid maxillary expanders. Am J Orthod Dentofac Orthop 2016;149:331–8.

[2] Palomares NB, Celeste RK, Oliveira BH De, Miguel JAM. How does orthodontic treatment affect young adults' oral health-related quality of life? Am J Orthod Dentofac Orthop 2012;141:751–8.

[3] Kolawole KA, Agbaje HO, Otuyemi OD. Impact of malocclusion on oral health related quality of life of final year dental students. Odontostomatol 2014;37:64–74.

[4] Fournier a, Payant L, Bouclin R. Adherence of *Streptococcus mutans* to orthodontic brackets. Am J Orthod Dentofacial Orthop 1998;114:414–7.

[5] Nascimento LEAG do, Pithon MM, dos Santos RL, Ayres Freitas AO, Sales Alviano D, Nojima LI, et al. Colonization of *Streptococcus mutans* on

esthetic brackets: Self-ligating vs conventional. Am J Orthod Dentofac Orthop 2013;143:S72–7.

[6] Zheng Y, Li Z, He X. Influence of fixed orthodontic appliances on the change in oral Candida strains among adolescents. J Dent Sci 2016;11:17–22.

[7] Eissaa OE, El-Shourbagy EM, Ghobashy SA. *In vivo* effect of a fluoride releasing adhesive on inhibition of enamel demineralization around orthodontic brackets. Tanta Dent J 2013;10:86–96.

[8] Benkaddour A, Bahije L, Bahoum A, Zaoui F. L'orthodontie et les déminéralisations amélaires : étude clinique des facteurs de risque. Int Orthod 2014;12:458–66.

[9] Zhang N, Weir MD, Chen C, Melo MAS, Bai Y, Xu HHK. Orthodontic cement with protein-repellent and antibacterial properties and the release of calcium and phosphate ions. J Dent 2016;50:51–9.

[10] Westphal Theile C, Strauss S, Northridge ME, Birenz S. The oral healthcare manager in a patient-centered health facility. J Evid Based Dent Pract 2016;16:34–42.

[11] Kregiel D. Advances in biofilm control for food and beverage industry using organo-silane technology: A review. Food Control 2014;40:32–40.

[12] Gottenbos B, Van Der Mei HC, Klatter F, Nieuwenhuis P, Busscher HJ. *In vitro* and *in vivo* antimicrobial activity of covalently coupled quaternary ammonium silane coatings on silicone rubber. Biomaterials 2002;23:1417–23.

[13] Kickelbick G. Concepts for the incorporation of inorganic building blocks into organic polymers on a nanoscale. Prog. Polym. Sci. 2003;28:83–114.

[14] Schmidt H. New type of non-crystalline solids between inorganic and organic materials. J Non Cryst Solids 1985;73:681–91.

[15] Ferreira FAS, Amaral T, Ysnaga OAE, Pereira-da-Silva MA, Lopes JH, Lewicki JP, et al. Structure–property relationship of new polyimide–organically modified silicate–phosphotungstic acid hybrid material system. J Mater Sci 2016;51:4815–24.

[16] Pandey PC. Review on ormosil-based biomaterials and their applications in sensor design. J Indian Inst Sci 1999;79:415–30.

[17] Tripathi VS, Kandimalla VB, Ju H. Preparation of ormosil and its applications in the immobilizing biomolecules. Sensors Actuators, B Chem 2006;114:1071–82.

[18] Mackenzie, John D, Bescher, Eric P. Structures , Properties and Potential Applications of Ormosils. J Sol-Gel Sci Technol 1998;377:371–7.

[19] Gong SQ, Epasinghe DJ, Zhou B, Niu LN, Kimmerling KA, Rueggeberg FA, et al. Effect of water-aging on the antimicrobial activities of an ormosil-containing orthodontic acrylic resin. Acta Biomater 2013;9:6964–73.

[20] Nagamune H, Maeda T, Ohkura K, Yamamoto K, Nakajima M, Kourai H. Evaluation of the cytotoxic effects of bis-quaternary ammonium antimicrobial reagents on human cells. Toxicol Vitr 2000;14:139–47.

[21] Imazato S, Chen J hua, Ma S, Izutani N, Li F. Antibacterial resin monomers based on quaternary ammonium and their benefits in restorative dentistry. Jpn Dent Sci Rev 2012;48:115–25.

[22] Liu Y, Cui X, Hao C, Tao F, Li J. Modified gelatin with quaternary ammonium salts containing epoxide groups. Chinese Chem Lett 2014;25:1193–7.

[23] Melo MAS, Wu J, Weir MD, Xu HHK. Novel antibacterial orthodontic cement containing quaternary ammonium monomer dimethylaminododecyl methacrylate. J Dent 2014;42:1193–201.

[24] Gong SQ, Niu L-NN, Kemp LK, Yiu CKY, Ryou H, Qi Y-PP, et al. Quaternary ammonium silane-functionalized, methacrylate resin composition with antimicrobial activities and self-repair potential. Acta Biomater 2012;8:3270–82.

[25] Munhoz-Bonilla, Fernández-García M. The roadmap of antimicrobial polymeric materials in macromolecular nanotechnology. Eur Polym J 2015;65:46–62.

[26] Palermo EF, Lee D, Ramamoorthy A, Kuroda K. Role of cationic group structure in membrane binding and disruption by amphiphilic copolymers. J Phys Chem B 2011;115:366–75.

[27] Li F, Weir MD, Xu HHK. Effects of quaternary ammonium chain length on antibacterial bonding agents. J Dent Res 2013;92:932–8.

[28] Gong S, Epasinghe J, Rueggeberg FA, Niu L, Mettenberg D, Yiu CKYY, et al. An ormosil-containing orthodontic acrylic resin with concomitant improvements in antimicrobial and fracture toughness properties. PLoS One 2012;7:e42355.

[29] Rueggeberg FA, Hashinger DT, Fairhurst CW. Calibration of FTIR conversion analysis of contemporary dental resin composites. Dent Mater 1990;6:241–9.

[30] Atai M, Watts DC. A new kinetic model for the photopolymerization shrinkage-strain of dental composites and resin-monomers. Dent Mater 2006;22:785–91.

[31] Gao B, Qi C, Liu Q. Immobilization of quaternary ammonium salts on grafting particle polystyrene/SiO2 and preliminary study of application performance. Appl Surf Sci 2008;254:4159–65.

[32] Shah KJ, Mishra MK, Shukla AD, Imae T, Shah DO. Controlling wettability and hydrophobicity of organoclays modified with quaternary ammonium surfactants. J Colloid Interface Sci 2013;407:493–9.

[33] Pigorsch E. Spectroscopic Characterisation of Cationic Quaternary Ammonium Starches. Starch - Stärke 2009;61:129–38.

[34] Kong Z, Wei J, Li Y, Liu N, Zhang H, Zhang Y, et al. Rapid removal of Cr (VI) ions using Quaternary ammonium fibers functioned by 2- (dimethylamino) ethyl methacrylate and modified with 1-bromoalkanes. Chem Eng J 2014;254:365–73.

[35] Son M, Ha Y, Choi M-C, Lee T, Han D, Han S, et al. Microstructure and properties of polyamideimide/silica hybrids compatibilized with 3-aminopropyltriethoxysilane. Eur Polym J 2008;44:2236–43.

[36] Khalil M, Saeed S, Ahmad Z. Mechanical and Thermal Properties of Polyimide / Silica Hybrids with Imide-Modified Silica Network Structures 2007.

[37] He Y, Heine E, Keusgen N, Keul H, Möller M. Synthesis and characterization of amphiphilic monodisperse compounds and poly(ethylene imine)s: Influence of their microstructures on the antimicrobial properties. Biomacromolecules 2012;13:612–23.